Discrete Exterior Calculus Discretization of the Incompressible Navier-Stokes Equations

Mamdouh M. Mohamed (Post-doc, ME, PSE Division)
Ravi Samtaney (ME, PSE Division)
Anil N. Hirani (Dept. of Math, UIUC)

King Abdullah University of Science and Technology

Discovery through simulation

July 30, 2015

Outline

- Motivation.
- Navier-Stokes equations in differential geometry notation.
- Discrete Exterior Calculus.
- 2D discretization of Navier-Stokes equations.
- Numerical examples.
- Conclusion.

Motivation

Fidelity measures of a numerical discretization method.

- Numerical fidelity: **convergence** and **stability** indicate how well the mathematics of the PDE are represented by the numerical method.
- Physical fidelity: how well the physics of the system are preserved by the numerical method.
- Preserving the key physical quantities during the numerical solution is important to avoid non-physical numerical artefacts.

Motivation

Key physical quantities to preserve:

- Conservation of primary quantities: mass and momentum.
- Conservation of secondary quantities:[J. Perot, Annu. Rev. Fluid Mech. 2011]
  - Vorticity: Important for turbulence and shallow water simulations.
  - Kinetic energy: Important for large-eddy simulation of turbulent flow.
  - Entropy: Important for compressible flow simulations.

Motivation

Examples of mumerical methods with conservation properties.

- Mass:
  - Finite volume method.
  - Classic finite element method.
  - Discontiuous Galerkin method.
  - Staggered mesh methods on Cartesian meshes.
  - Covolume method on unstructured meshes.
- Vorticity:
  - Staggered mesh methods on Cartesian meshes.
  - Covolume method on unstructured meshes.
- Kinetic energy:
  - Staggered mesh methods on Cartesian meshes.
  - Covolume method on unstructured meshes.

KAUST
King Abdullah University of Science and Technology

The covolume method

- The covolume method, originally introduced by Nicolaides (1989) and Hall et al. (1991), is a low order method that is free of spurious modes.
- The covolume method convergence was estimated by Nicolaides (1992) to be of second order rate for structured/semi-structured meshes and first order accurate otherwise.

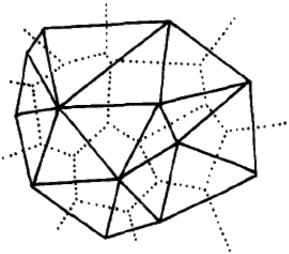

The covolume method

- The local/global conservation properties of the covolume method were later revealed by Perot (2000).
- The conservative behavior of the covolume method is attributed to the discrete differential operators that mimic the behavior of their smooth counterparts.
- The resulting discrete system can be manipulated into discrete conservation statements for key physical quantities.
- The covolume method conserves mass, momentum, vorticity and kinetic energy.

KAUST
King Abdullah University of Science and Technology

Discrete Exterior Calculus Discretizations

- In computer graphics some the Discrete Exterior Calculus (**DEC**) approach to simulate incompressible flows.
- The developed discretizations [Elcott et. al (2007) and Mullen et. al (2009)] have similarities with the covolume method, but are applicable on both flat/curved surfaces.
- The convective term is approximated through finite-volume-based or back tracing of characteristics and interpolation schemes.
- Little quantitative analysis of the scheme performance is presented.

Objective

1. Use Discrete Exterior Calculus (DEC) to derive a conservative discretization of incompressible Navier-Stokes equations that is applicable for 2D flat/curved and 3D domains with unstructured meshes.
2. Conduct quantitative analysis for numerical convergence and conservation.

$$\boxed{\begin{aligned}\frac{\partial \mathbf{u}}{\partial t} - \mu\Delta\mathbf{u} + (\mathbf{u}.\nabla)\mathbf{u} + \nabla p = 0\\ \nabla.\mathbf{u} = 0\end{aligned}}$$

Using the vector identities:

$$\Delta\mathbf{u} = \nabla(\nabla.\mathbf{u}) - \nabla\times(\nabla\times\mathbf{u})$$

$$(\mathbf{u}.\nabla)\mathbf{u} = \frac{1}{2}\nabla(\mathbf{u}.\mathbf{u}) - \mathbf{u}\times(\nabla\times\mathbf{u})$$

Define the dynamic pressure: $p^d = p + \frac{1}{2}(\mathbf{u}.\mathbf{u})$

$$\boxed{\begin{aligned}&\frac{\partial \mathbf{u}}{\partial t} + \mu\nabla\times\nabla\times\mathbf{u} - \mathbf{u}\times(\nabla\times\mathbf{u}) + \nabla p^d = 0\\ &\nabla.\mathbf{u} = 0\end{aligned}}$$

Navier-Stokes Equations in Differential Geometry Notation

$$\boxed{\begin{aligned}&\frac{\partial \mathbf{u}}{\partial t} + \mu \nabla \times \nabla \times \mathbf{u} - \mathbf{u} \times (\nabla \times \mathbf{u}) + \nabla p^d = 0\\ &\nabla . \mathbf{u} = 0\end{aligned}}$$

For any vector field $\mathbf{u}$ and a scalar field f:

$$\begin{aligned}(\nabla \times \nabla \times \mathbf{u})^\flat &= (-1)^{N+1} * \mathrm{d} * \mathrm{d}\mathbf{u}^\flat,\\ (\mathbf{u} \times (\nabla \times \mathbf{u}))^\flat &= (-1)^{N+1} * (\mathbf{u}^\flat \wedge *\mathrm{d}\mathbf{u}^\flat),\\ (\nabla . \mathbf{u})^\flat &= *\mathrm{d} * \mathbf{u}^\flat,\\ (\nabla f)^\flat &= \mathrm{d}f\end{aligned}$$

$$\boxed{\begin{aligned}&\frac{\partial \mathbf{u}^\flat}{\partial t} + (-1)^{N+1} \mu * \mathrm{d} * \mathrm{d}\mathbf{u}^\flat + (-1)^{N+2} * (\mathbf{u}^\flat \wedge *\mathrm{d}\mathbf{u}^\flat) + \mathrm{d}p^d = 0,\\ &* \mathrm{d} * \mathbf{u}^\flat = 0\end{aligned}}$$

KAUST
King Abdullah University of Science and Technology

An Alternative Derivation

Starting from Navier-Stokes equation in coordinate invariant form (See Abraham, Marsden, Ratiu, "Manifolds, Tensor Analysis and Applications")

$$\boxed{\frac{\partial \mathbf{u}^\flat}{\partial t} + \mu(\delta \mathrm{d} + \mathrm{d}\delta)\mathbf{u}^\flat + \pounds_{\mathbf{u}}\mathbf{u}^\flat - \frac{1}{2}\mathrm{d}(\mathbf{u}^\flat(\mathbf{u})) + \mathrm{d}p = 0}$$

where δ is the codifferential operator defined as $\delta = (-1)^{N(k-1)+1} * \mathrm{d} *$.

Using Cartan homotopy formula:

$$\pounds_{\mathbf{u}}\mathbf{u}^\flat = \mathrm{d}i_{\mathbf{u}}\mathbf{u}^\flat + i_{\mathbf{u}}\mathrm{d}\mathbf{u}^\flat = \mathrm{d}(\mathbf{u}^\flat(\mathbf{u})) + i_{\mathbf{u}}\mathrm{d}\mathbf{u}^\flat$$

$$\boxed{\frac{\partial \mathbf{u}^\flat}{\partial t} + \mu\delta\mathrm{d}\mathbf{u}^\flat + i_{\mathbf{u}}\mathrm{d}\mathbf{u}^\flat + \frac{1}{2}\mathrm{d}(\mathbf{u}^\flat(\mathbf{u})) + \mathrm{d}p = 0.}$$

An Alternative Derivation: Cont.

$$\boxed{\frac{\partial \mathbf{u}^\flat}{\partial t} + \mu\delta \mathrm{d}\mathbf{u}^\flat + i_{\mathbf{u}}\mathrm{d}\mathbf{u}^\flat + \frac{1}{2}\mathrm{d}(\mathbf{u}^\flat(\mathbf{u})) + \mathrm{d}p = 0.}$$

- Defining the dynamic pressure 0-form as $p^d = p + \frac{1}{2}(\mathbf{u}^\flat(\mathbf{u}))$.
- Substitute with $\delta = (-1)^{N+1} * \mathrm{d} *$.
- Substitute for the contraction with [A. Hirani, PhD Dissertation, Caltech (2003)]

$$i_{\mathbf{x}}\alpha = (-1)^{k(N-k)} * (*\alpha \wedge \mathbf{x}^\flat)$$

$$\boxed{\frac{\partial \mathbf{u}^\flat}{\partial t} + (-1)^{N+1}\mu * \mathrm{d} * \mathrm{d}\mathbf{u}^\flat + (-1)^{N-2} * (\mathbf{u}^\flat \wedge *\mathrm{d}\mathbf{u}^\flat) + \mathrm{d}p^d = 0.}$$

Applying the exterior derivative (d) to the above equation

$$\boxed{\frac{\partial \mathrm{d}\mathbf{u}^\flat}{\partial t} + (-1)^{N+1}\mu\mathrm{d} * \mathrm{d} * \mathrm{d}\mathbf{u}^\flat + (-1)^{N}\mathrm{d} * (\mathbf{u}^\flat \wedge *\mathrm{d}\mathbf{u}^\flat) = 0.}$$

Domain Discretization

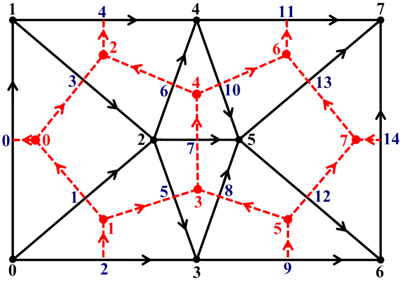

- The domain Ω is approximated by the simplicial complex K.
- A k-simplex is denoted by $\sigma^k = [v_0, ..., v_k] \in K$.
- The circumcentric dual to the simplicial complex K is the dual complex $\star K$.
- For a primal k-simplex $\sigma^k \in K$, its dual is an $(N - k)$-cell denoted by $\star\sigma^k \in \star K$

- The DEC operators (e.g. exterior derivative, Hodge star, wedge product, etc) have the advantage that they satisfy the same rules/identities that characterizes their smooth counterparts.
- Such mimetic behavior of the discrete operators is known to result in preserving the physics implied in the smooth governing equations at the discrete level.

- Discrete differential forms: a discrete form can be thought as the integration of the smooth form over a discrete mesh object; i.e. line, area or volume.
- For example, for the smooth velocity 1-form $\mathbf{u}^\flat$, its discretization can be defined:
  - on primal edges σ^1 as $v = \int_{\sigma^1} \mathbf{u}\ d\mathbf{l}$.
  - on dual edges $\star\sigma^1$ as $u = \int_{\star\sigma^1} \mathbf{u}\ d\mathbf{l}$.

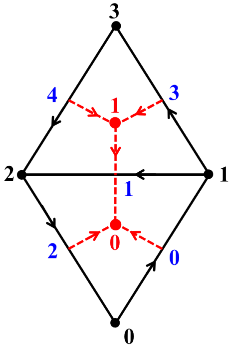

The space of discrete k-forms defined on primal and dual mesh complexes is denoted by $C^k(K)$ and $D^k(\star K)$, respectively.

$$
\begin{array}{ccccc}
C^0(K) & \xrightarrow{\mathrm{d}_0} & C^1(K) & \xrightarrow{\mathrm{d}_1} & C^2(K) \\
\Big\downarrow *_0 & & \Big\downarrow *_1 & & \Big\downarrow *_2 \\
D^2(\star K) & \xleftarrow{-\mathrm{d}_0^T} & D^1(\star K) & \xleftarrow{\mathrm{d}_1^T} & D^0(\star K)
\end{array}
$$

$$
\begin{array}{ccccccc}
C^0(K) & \xrightarrow{\mathrm{d}_0} & C^1(K) & \xrightarrow{\mathrm{d}_1} & C^2(K) & \xrightarrow{\mathrm{d}_2} & C^3(K) \\
\Big\downarrow *_0 & & \Big\downarrow *_1 & & \Big\downarrow *_2 & & \Big\downarrow *_3 \\
D^3(\star K) & \xleftarrow{\mathrm{d}_0^T} & D^2(\star K) & \xleftarrow{\mathrm{d}_1^T} & D^1(\star K) & \xleftarrow{\mathrm{d}_2^T} & D^0(\star K)
\end{array}
$$

$$\mathrm{d}_0\beta = \begin{bmatrix} -1 & 1 & 0 & 0 \\ 0 & -1 & 1 & 0 \\ 1 & 0 & -1 & 0 \\ 0 & -1 & 0 & 1 \\ 0 & 0 & 1 & -1 \end{bmatrix} \begin{bmatrix} \beta_0 \\ \beta_1 \\ \beta_2 \\ \beta_3 \end{bmatrix}$$

$$\mathrm{d}_1 = \begin{bmatrix} 1 & 1 & 1 & 0 & 0 \\ 0 & -1 & 0 & 1 & 1 \end{bmatrix}$$

$$\star_1 = \begin{bmatrix} \frac{|\star\sigma_0^1|}{|\sigma_0^1|} & 0 & 0 & 0 & 0 \\ 0 & \frac{|\star\sigma_1^1|}{|\sigma_1^1|} & 0 & 0 & 0 \\ 0 & 0 & \frac{|\star\sigma_2^1|}{|\sigma_2^1|} & 0 & 0 \\ 0 & 0 & 0 & \frac{|\star\sigma_3^1|}{|\sigma_3^1|} & 0 \\ 0 & 0 & 0 & 0 & \frac{|\star\sigma_4^1|}{|\sigma_4^1|} \end{bmatrix}$$

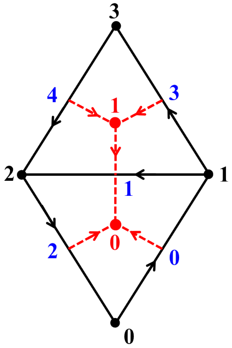

For the discrete wedge product, we use the definition in [Hirani Ph.D. dissertation (2003)] for primal-primal wedge product:

The wedge product between a discrete primal 1-form α and a discrete primal 0-form β defined over a primal edge $[0,1]$ is

$$\langle \alpha \wedge \beta, [0,1] \rangle = \frac{1}{2} \langle \alpha, [0,1] \rangle (\langle \beta, [0] \rangle + \langle \beta, [1] \rangle).$$

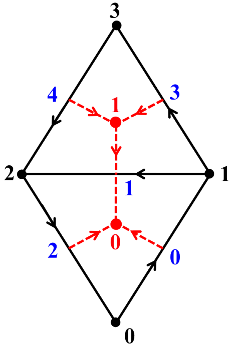

The discrete wedge product expression for the whole mesh:

$$\frac{1}{2} \begin{bmatrix} \alpha_0 & \alpha_0 & 0 & 0 \\ 0 & \alpha_1 & \alpha_1 & 0 \\ \alpha_2 & 0 & \alpha_2 & 0 \\ 0 & \alpha_3 & 0 & \alpha_3 \\ 0 & 0 & \alpha_4 & \alpha_4 \end{bmatrix} \begin{bmatrix} \beta_0 \\ \beta_1 \\ \beta_2 \\ \beta_3 \end{bmatrix}$$

2D Discretization

The discretization of NS equations is carried out here following the exact fractional step method [Hall et. al (1991), Chang et. al (2002)], consisting of two steps:

1. The discretization is carried out for the vorticity form of Navier-Stokes equations.
2. Substitute the velocity by its definition as the curl of a stream function.

$$\boxed{\frac{\partial \mathrm{d}\mathbf{u}^\flat}{\partial t} + (-1)^{N+1}\mu \mathrm{d} * \mathrm{d} * \mathrm{d}\mathbf{u}^\flat + (-1)^N \mathrm{d} * (\mathbf{u}^\flat \wedge *\mathrm{d}\mathbf{u}^\flat) = 0.}$$

$$\begin{tikzcd}
C^0(K) \arrow[r, "\mathrm{d}_0"] \arrow[d, "*_0"] & C^1(K) \arrow[r, "\mathrm{d}_1"] \arrow[d, "*_1"] & C^2(K) \arrow[d, "*_2"] \\
D^2(\star K) & D^1(\star K) \arrow[l, "-\mathrm{d}_0^T"'] & D^0(\star K) \arrow[l, "\mathrm{d}_1^T"']
\end{tikzcd}$$

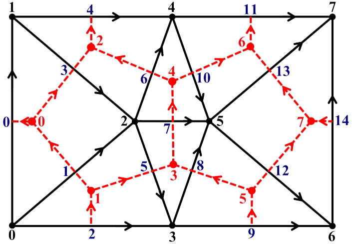

$$\boxed{\begin{aligned} -\mathrm{d}_0^T \frac{U^{n+1} - U^n}{\Delta t} &+ \mu \mathrm{d}_0^T *_1 \mathrm{d}_0 *_0^{-1} \left[-\mathrm{d}_0^T U + \mathrm{d}_b V\right] \\ &- \mathrm{d}_0^T *_1 W_v *_0^{-1} \left[-\mathrm{d}_0^T U + \mathrm{d}_b V\right] = 0. \end{aligned}}$$

The discrete representation of the continuity equation is:

$$\star_2 \mathrm{d}_1 \star_1^{-1} U = 0$$

U is in the null space of $[\star_2 \mathrm{d}_1 \star_1^{-1}]$.

$$[\star_2 \mathrm{d}_1 \star_1^{-1}][\star_1 \mathrm{d}_0] = \star_2 \mathrm{d}_1 \mathrm{d}_0 = 0$$

The vector U can uniquely be expressed in terms of the basis $[\star_1 \mathrm{d}_0]$

$$U = \star_1 \mathrm{d}_0 \Psi$$

$$\boxed{\begin{aligned} -\mathrm{d}_0^T \frac{U^{n+1} - U^n}{\Delta t} + \mu \mathrm{d}_0^T \ast_1 \mathrm{d}_0 \ast_0^{-1} \left[-\mathrm{d}_0^T U + \mathrm{d}_b V \right] \\ - \mathrm{d}_0^T \ast_1 W_v \ast_0^{-1} \left[-\mathrm{d}_0^T U + \mathrm{d}_b V \right] = 0. \end{aligned}}$$

Substitute with $U = \ast_1 \mathrm{d}_0 \Psi$

$$\boxed{\begin{aligned} -\frac{1}{\Delta t} \mathrm{d}_0^T \ast_1 \mathrm{d}_0 \Psi^{n+1} - \mu \mathrm{d}_0^T \ast_1 \mathrm{d}_0 \ast_0^{-1} \mathrm{d}_0^T \ast_1 \mathrm{d}_0 \Psi \\ + \mathrm{d}_0^T \ast_1 W_v \ast_0^{-1} \mathrm{d}_0^T \ast_1 \mathrm{d}_0 \Psi = F. \end{aligned}}$$

$$F = \frac{1}{\Delta t} \mathrm{d}_0^T U^n - \mu \mathrm{d}_0^T \ast_1 \mathrm{d}_0 \ast_0^{-1} \mathrm{d}_b V + \mathrm{d}_0^T \ast_1 W_v \ast_0^{-1} \mathrm{d}_b V$$

2D Discretization: Cont.

The linear system is solved in two steps as a predictor-corrector method.

1. First, we advance the system explicitly by a half time step

$$\boxed{\begin{aligned}&\left[-\frac{1}{0.5\Delta t}\mathrm{d}_0^T *_1 \mathrm{d}_0\right]\Psi^{n+\frac{1}{2}}\\ &= F + \left[\mu \mathrm{d}_0^T *_1 \mathrm{d}_0 *_0^{-1} \mathrm{d}_0^T - \mathrm{d}_0^T *_1 W_v^n *_0^{-1} \mathrm{d}_0^T\right] U^n\end{aligned}}$$

$$\Psi^{n+\frac{1}{2}} \quad \Rightarrow \quad U^{n+\frac{1}{2}} = *_1 \mathrm{d}_0 \Psi^{n+\frac{1}{2}} \quad \Rightarrow \quad W_v^{n+\frac{1}{2}}$$

2. Then solve the linear system semi-implicitly

$$\boxed{\begin{aligned}&[-\frac{1}{\Delta t}\mathrm{d}_0^T *_1 \mathrm{d}_0 - \mu \mathrm{d}_0^T *_1 \mathrm{d}_0 *_0^{-1} \mathrm{d}_0^T *_1 \mathrm{d}_0\\ &+ \mathrm{d}_0^T *_1 W_v^{n+\frac{1}{2}} *_0^{-1} \mathrm{d}_0^T *_1 \mathrm{d}_0]\Psi^{n+1} = F\end{aligned}}$$

The evaluation of the tangential velocity at $(n+\frac{1}{2})$ was shown [Perot (2000)] to be necessary for kinetic energy conservation.

$$U = \star_1 \mathrm{d}_0 \Psi$$

The discrete continuity equation is:

$$\star_2 \mathrm{d}_1 \star_1^{-1} U = 0$$

$$[\star_2 \mathrm{d}_1 \star_1^{-1}][\star_1 \mathrm{d}_0]\Psi = \star_2 \mathrm{d}_1 \mathrm{d}_0 \Psi = 0$$

The developed formulation guarantees the mass conservation up to the machine precision, regardless of the error incurred during the linear system solution.

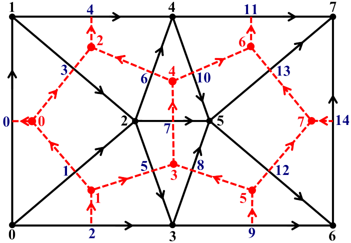

Conservation Properties: Vorticity conservation

$$-\frac{\mathrm{d}_0^T U^{n+1} - \mathrm{d}_0^T U^n}{\Delta t} + \mu \mathrm{d}_0^T *_1 \mathrm{d}_0 *_0^{-1} [-\mathrm{d}_0^T U] - \mathrm{d}_0^T *_1 W_v *_0^{-1} [-\mathrm{d}_0^T U] = 0$$

$$-\frac{\mathrm{d}_0^T U^{n+1} - \mathrm{d}_0^T U^n}{\Delta t} + \mu \mathrm{d}_0^T [*_1 \mathrm{d}_0 X] - \mathrm{d}_0^T [*_1 W_v X] = 0$$

- The vorticity out-flux from a dual cell boundary is exactly equal to the vorticity in-flux to the neighboring dual cell.
- The vorticity is conserved locally and globally up to the machine precision.

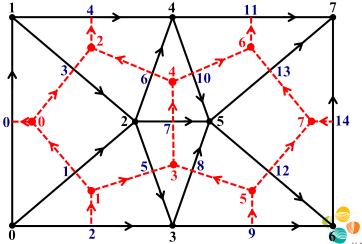

How this discretization is different?

- The discretization is entirely based on the DEC framework.
- The discretization is similar to some of the covolume method discretizations only for the special case of 2D structured triangular mesh on flat domains, but different otherwise.
- Unlike all covolume discretizations, the current discretization is capable of simulating flows over both flat and curved surfaces.

- The driven cavity flow is simulated at $Re = 1000$.
- The simulations are carried out on a Delaunay mesh and a structured-triangular mesh with 32482 and 32258 elements, respectively $\rightarrow$ almost the same resolution as a 128×128 Cartesian mesh.
- The time step $\Delta t = 0.1$, and the steady solution is attained at almost $T = 100$.

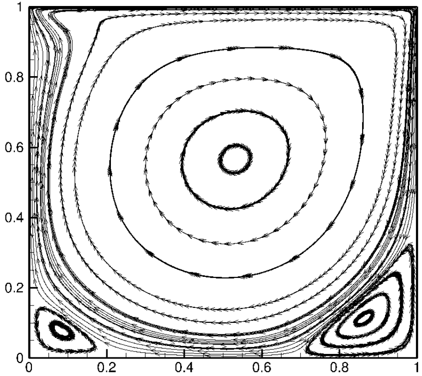

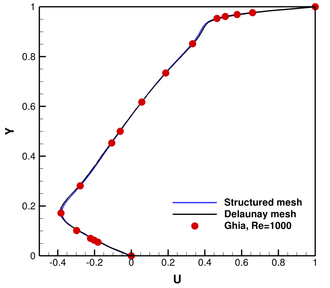

Figure: Cross-section of the steady velocity profile ($T = 100$) at the two domain center lines for driven cavity test case at Reynolds number = 1000. The simulation results are compared with Ghia (1982).

Results: Taylor-Green vortices

- The decay of Taylor-Green vortices with time has an analytical solution that for the 2D case is expressed as

$$u_x = -cos(x)sin(y)e^{-2\nu t}$$
$$u_y = sin(x)cos(y)e^{-2\nu t}$$

- The simulation is conducted using a Delaunay mesh consisting of 50852 elements, a time step $\Delta t = 0.1$ and kinematic viscosity $\nu = 0.01$.
- Periodic boundary conditions applied on all domain boundaries.

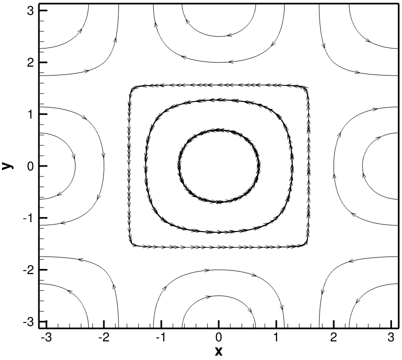

Results: Taylor-Green vortices

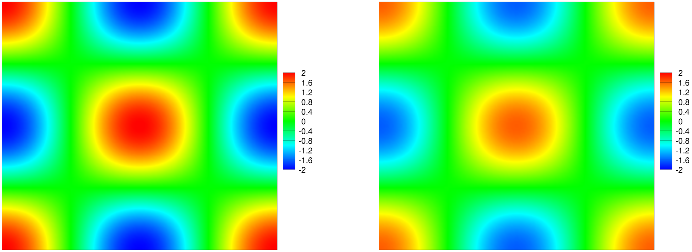

:	:

Figure: The vorticity contour plot for Taylor-Green vortices at time (a) $T = 0$, (b) $T = 10$.

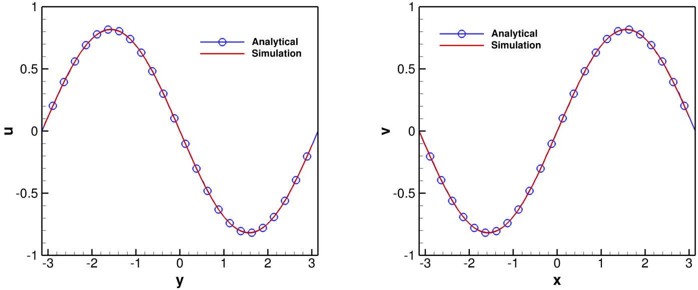

Figure: Cross-section of the velocity x and y-components profile at the two domain center lines for Taylor-Green vortices at time $T = 10$.

Results: Poiseuille flow

- The Poiseuille flow has a steady analytical solution in a unit square with $\mu = 1.0$

$$u_x = y(1-y), \quad u_y = 0$$

- The L^2-norm of the velocity 1-form (u) error is calculated according to Hall et al.(1991) as

$$\|u^{exact} - u\| = \left[\sum_{\sigma^1} (u^{exact} - u)^2 |\sigma^1| \, |\star\sigma^1|\right]^{1/2}$$

- The simulation is carried out for structured-triangular, Delaunay and well-centered meshes of different resolutions.

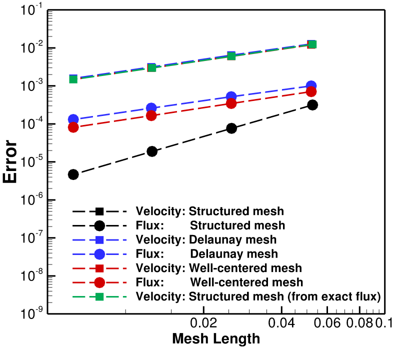

- The velocity 1-form u (flux) convergence is of a second order rate for the structured-triangular mesh case, and with a first order rate unstructured meshes.
- The velocity vector converges in the first order fashion due to its first order interpolation scheme.

Results: Double shear layer

- The initial flow for double shear layer represents a shear layer of finite thickness with a small magnitude of vertical velocity perturbation

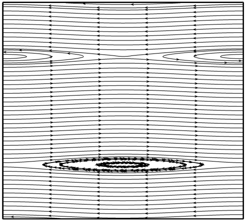

$$u_x = \begin{cases} \tanh((y-0.25)/\rho), & \text{for } y \le 0.5, \\ \tanh((0.75-y)/\rho), & \text{for } y > 0.5, \end{cases}$$

$$u_y = \delta \sin(2\pi x)$$

with $\rho = 1/30$ and $\delta = 0.05$.

- The simulation is carried out for an inviscid flow ($\mu = 0$).
- Five simulations are conducted using a time step of $\Delta t = 0.001$ on structured-triangular meshes with number of elements equal to 3042, 12482, 32258, 50562 and 204800.
- Periodic boundary conditions applied on all domain boundaries.

Results: Double shear layer

Results: Double shear layer

- The kinetic energy is calculated as $\int_\Omega \mathbf{u}.\mathbf{u}\ d\Omega$.
- The relative kinetic energy error $\left(\frac{KE(0)-KE(T)}{KE(0)}\right)$ is calculated at simulation time $T = 2.0$.

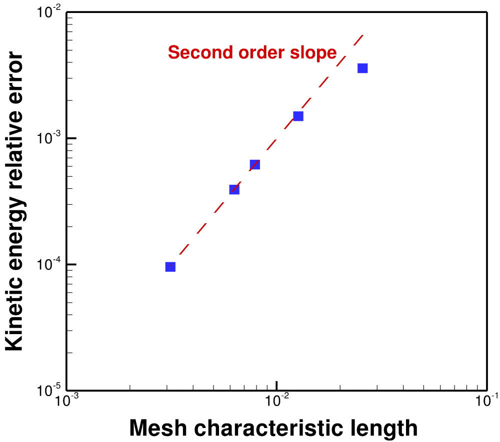

Results: Taylor vortices

- The vorticity distribution for each Taylor vortex is expressed as [A. McKenzie, PhD Dissertation, CalTech (2007)]

$$\omega(x,y) = \frac{G}{a}\left(2 - \frac{r^2}{a^2}\right)\exp\left(0.5\left(1 - \frac{r^2}{a^2}\right)\right)$$

with $G = 1.0$, $a = 0.3$.

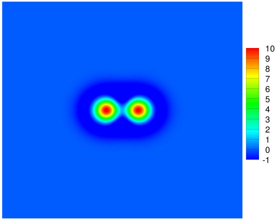

- The domain is initialized with two vortices separated by a distance of 0.8.
  - The simulations are carried out for an inviscid flow ($\mu = 0$) on a mesh consisting of 132204 equilateral triangular element, using various time steps in the range $[1.0 - 0.002]$.
  - Periodic boundary conditions applied on all domain boundaries.

Results: Taylor vortices

Results: Taylor vortices

The relative kinetic energy error ($\frac{KE(0)-KE(T)}{KE(0)}$) is calculated at simulation time $T = 20.0$.

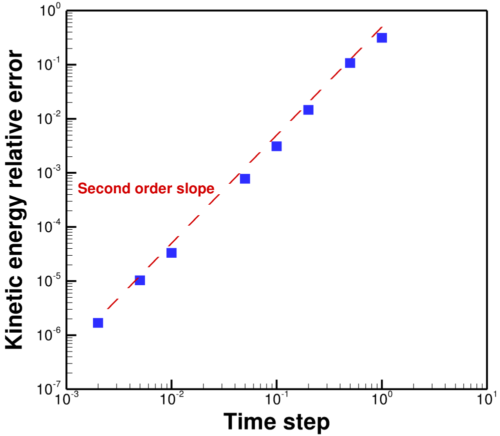

Results: Vortex leapfrogging

Results: Taylor vortices on a spherical surface

- A unit sphere surface is initialized with two vortices, separated by a distance of 0.4, having the distribution

$$\omega(x,y) = \frac{G}{a}\left(2 - \frac{r^2}{a^2}\right)\exp\left(0.5\left(1 - \frac{r^2}{a^2}\right)\right)$$

with $G = 0.5$, $a = 0.1$.

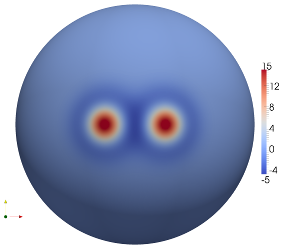

  - The simulation is carried out for an inviscid flow ($\mu = 0$) using a mesh containing 327680 triangular elements, with various time steps in the range $[1.0 - 0.05]$.

Results: Taylor vortices on a spherical surface

Results: Taylor vortices on a spherical surface

The relative kinetic energy error ($\frac{KE(0)-KE(T)}{KE(0)}$) is calculated at simulation time $T = 10.0$.

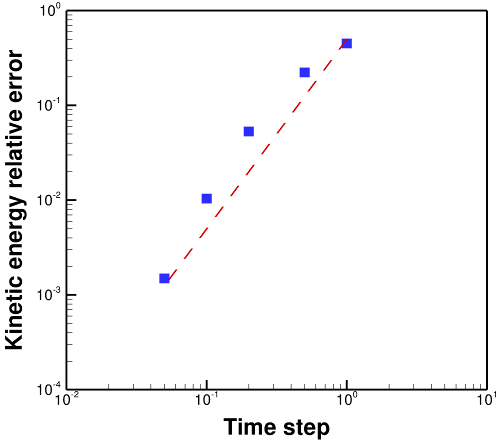

Results: Vortices ring on a spherical surface

- Consider N equidistant point vortices, having the same strength, positioned on a circle with fixed latitude on a spherical surface .[Polvani et. al (1993)].
- It was shown analytically that the vortices will rotate around the z-axis in a stable fashion given that the circle's latitude $\theta < \theta_c$ and the number of vortices $N \leq 7$.
- For $N = 6$, the critical polar angle $\theta_c \sim 0.464$.

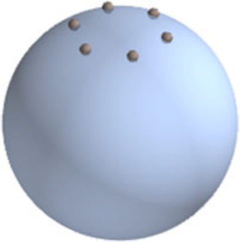

Figure: [Vankerschaver et. al (2014)]

Results: Vortices ring on a spherical surface

- the point vortices are replaced with vortices having the distribution

$$\omega = \frac{\tau}{cosh^2(\frac{3r}{a})}$$

with $\tau = 3.0$ to be the vortex strength, $a = 0.15$ is the vortex radius.

- The vortices are placed on a unit sphere at latitude $\theta = 0.4$.
- The spherical surface is meshed with 81920 elements, and the simulation is conducted for an inviscid flow ($\mu = 0$) with a time step $\Delta t = 0.005$.

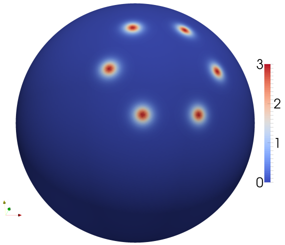

Results: Vortices ring on a spherical surface

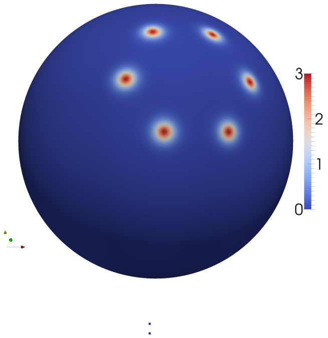

Figure: The vorticity contour plot for 6 vortices on a spherical surface at latitude $\theta = 0.4$ at time: (a) T=0.0 and (b) T=36.0.

The cyclic motion of the vortices can be captured by monitoring the relative solution change ($\frac{\|U(t)-U(0)\|}{\|U(0)\|}$) w.r.t. the initial solution.

The relative solution change $\left(\frac{\|U(t)-U(0)\|}{\|U(0)\|}\right)$.

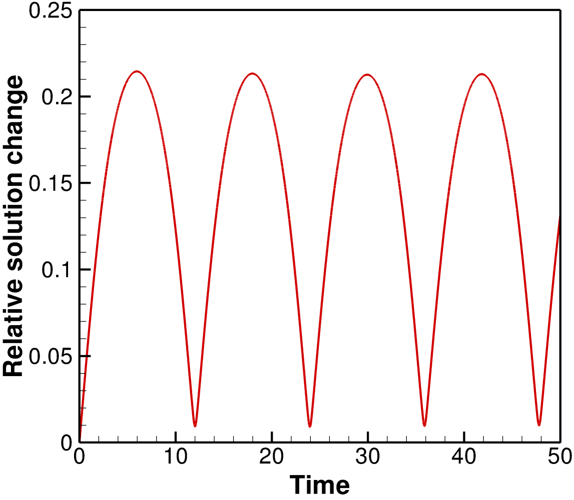

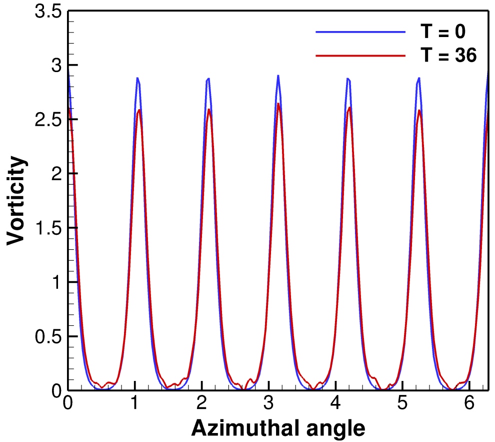

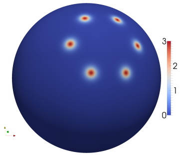

The relative change in the kinetic energy at time $T = 36$ is $\frac{KE(T{=}0) - KE(T{=}36)}{KE(T{=}0)} = 9.0 \times 10^{-6}$.

Conclusions

- A conservative discretization for NS equations was derived using DEC.
- The scheme converges with second order for structured/semi-structured meshes, and first order for otherwise unstructured meshes.
- The mass and vorticity were conserved up to machine precision for all conducted test cases.
- The kinetic energy converges with second order with the mesh size and time step for the tested cases on structured/semi-structured meshes.

KAUST
King Abdullah University of Science and Technology